



TITLE:

# A Note on the Theory of the Wind Tunnel Interference

AUTHOR(S):

HUDIMOTO, Busuke

---

CITATION:

HUDIMOTO, Busuke. A Note on the Theory of the Wind Tunnel Interference. *Memoirs of the Faculty of Engineering, Kyoto University* 1953, 15(1): 1-8

ISSUE DATE:

1953-03-31

URL:

<http://hdl.handle.net/2433/280271>

RIGHT:

# A Note on the Theory of the Wind Tunnel Interference

By

Busuke HUDIMOTO

Department of Applied Physics

(Received October, 1952)

The problem of the wind tunnel interference has long been studied and not a little is known about it<sup>1)</sup>. But recently, many experiments are made on the wing cascade, using a special kind of wind tunnels. And to obtain characteristics of the wing cascade, it is necessary to make corrections as to the theory of interference of these wind tunnels. In this paper, I have explained a fundamental theory based on the well-known method of correction, and then made a comparison with experimental results.

## 1. Theory

We assume, in this theory, a two-dimensional flow of inviscid fluid and will explain in the first place, the wind tunnel interference in the case of a boundary partly composed of solid walls and partly of free jet as shown in Fig. 1.

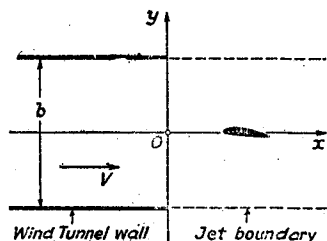


Fig. 1

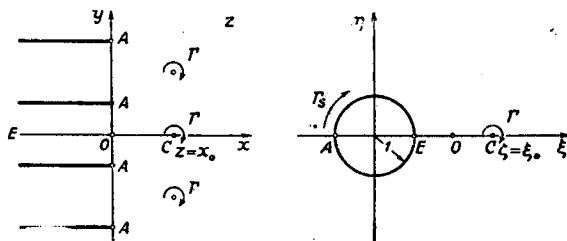


Fig. 2

Let the velocity of the flow far ahead of the aerofoil be  $V$ , and the breadth of the wind tunnel be  $b$ . Take  $x$ -axis along the tunnel axis bisecting the distance between the two solid walls and  $y$ -axis through the two edges of the solid walls, and assume that the aerofoil is situated at  $x_0$  and is expressed by a vortex of circulation  $\Gamma$ . To satisfy the boundary conditions, parallel and half-infinite solid planes passing through  $y = \frac{b}{2} + nb$ , ( $n = 1, \pm 2, \pm 3, \dots$ ) and a row of vortices situated at  $x = x_0$ ,  $y = nb$ , ( $n = \pm 1, \pm 2, \pm 3, \dots$ ), together with a

flow due to these vortices are also to be considered. But the deflection of the free jet caused by the aerofoil is assumed to be very small.

Let  $z=x+iy$  and  $\zeta=\xi+i\eta$ ;  $z$ -plane is transformed into  $\zeta$ -plane by the following relation:

$$z = \frac{b}{2\pi} \log \frac{1}{4} \left( \zeta - 2 + \frac{1}{\zeta} \right). \quad (1)$$

By this relation, the solid wall is transformed into a unit circle on  $\zeta$ -plane and point  $z=x_0$  corresponds to point  $\zeta=\xi_0$ .

Then, the complex velocity potential of the flow can be given by

$$F(z) = Vz + F_1(z), \quad (2)$$

$$F_1(\zeta) = \frac{i\Gamma}{2\pi} \log(\zeta - \xi_0) - \frac{i\Gamma}{2\pi} \log\left(\zeta - \frac{1}{\xi_0}\right) + \frac{i\Gamma_s}{2\pi} \log \zeta.$$

Circulation  $\Gamma_s$  is here added to avoid the infinite velocity at the edges of the solid walls, which is determined by the condition that the velocity at A on the  $\zeta$ -plane is zero, i. e.,

$$\Gamma_s = \Gamma \frac{\xi_0 - 1}{\xi_0 + 1}. \quad (3)$$

In the existence of solid walls, the velocity induced by the vortices except the one at  $z=x_0$  is given by the following relation;

$$\frac{dF_2(z)}{dz} = \frac{dF(z)}{dz} - \frac{i\Gamma}{2\pi} \cdot \frac{1}{z-x_0}.$$

and in the neighbourhood of  $z=x_0$ ,

$$\frac{dF_2}{dz} = \frac{i\Gamma}{b} f_1(x_0) + \frac{i2\pi\Gamma}{b} f_2(x_0) \Delta z + \dots, \quad (4)$$

where

$$\Delta z = z - x_0,$$

$$f_1(x_0) = \frac{1}{2} - \frac{2\xi_0}{(\xi_0+1)^2},$$

$$f_2(x_0) = \frac{1}{12} - \frac{2(\xi_0-1)}{(\xi_0+1)^2} - \frac{(\xi_0-1)^3}{(\xi_0+1)^3} + \frac{\xi_0^4-3}{(\xi_0+1)^4}.$$

Considering the case when the flat plate of chord length  $c$  is placed at an angle of incidence  $\alpha$  with the  $x$ -axis, the aerofoil is replaced by two vortices, one with circulation  $\Gamma_1$  at the  $c/4$ -point, and the other with circulation  $\Gamma_2$  at the mid-chord point. Let the positions of these two vortices be  $x_1$  and  $x_2$  respectively ( $x_2-x_1=\frac{c}{4}$ ), the velocity components  $u_0$  and  $v_0$  at the mid-chord point along the chord and normal to it, and  $u_1$  and  $v_1$ , the gradients of these velocity components, are as follows:

$$\begin{aligned}
 u_0 &= V \cos \alpha + \frac{\Gamma_1}{b} f_1(x_1) \sin \alpha + \frac{\Gamma_1 \pi c}{2b^2} f_2(x_1) \sin \alpha + \frac{\Gamma_2}{b} f_1(x_2) \sin \alpha, \\
 v_0 &= V \sin \alpha - \frac{\Gamma_1}{b} f_1(x_1) \cos \alpha - \frac{\Gamma_1 \pi c}{2b^2} f_2(x_1) \cos \alpha - \frac{\Gamma_2}{b} f_1(x_2) \cos \alpha, \\
 u_1 &= \frac{\Gamma_1 2\pi}{b^2} f_2(x_1) \sin \alpha + \frac{\Gamma_2 2\pi}{b^2} f_2(x_2) \sin \alpha, \\
 v_1 &= -\frac{\Gamma_1 2\pi}{b^2} f_2(x_1) \cos \alpha - \frac{\Gamma_2 2\pi}{b^2} f_2(x_2) \cos \alpha.
 \end{aligned} \tag{5}$$

The circulation  $\Gamma_0$  around a flat plate in an unlimited uniform flow is

$$\Gamma_0 = k\pi c V \sin \alpha,$$

where theoretically  $k=1$ , and, in the real fluid,  $k < 1$ .

In the present case, the magnitude of circulation  $\Gamma_1$  is determined by  $v_0$  and  $\Gamma_2$  by  $v_1$ , viz.  $\Gamma_1 = k\pi c v_0$  and  $\Gamma_2 = \frac{1}{4} k\pi c^2 v_1$ ,

$$\Gamma = \Gamma_1 + \Gamma_2 = k\pi c \left( v_0 + \frac{c}{4} v_1 \right). \tag{6}$$

Hence, neglecting small quantities,

$$\Gamma = \frac{k\pi c V \sin \alpha \left[ 1 - \frac{k}{2} \left( \frac{\pi c}{b} \right)^2 f_2(x_1) \right]}{1 + k \frac{\pi c}{b} f_1(x_1) + \frac{k}{2} \left( \frac{\pi c}{b} \right)^2 f_2(x_1)}, \tag{7}$$

and the lift  $L$  and the drag  $D$  are;

$$\begin{aligned}
 L &= \rho V \Gamma, \\
 D &= \rho \frac{\Gamma}{b} [\Gamma_1 f_1(x_1) + \Gamma_2 f_1(x_2)] + \rho \Gamma_1 \Gamma_2 \frac{\pi c}{2b^2} [f_2(x_1) - f_2(x_2)].
 \end{aligned} \tag{8}$$

In a special case when  $x_1 = x_2 = -\infty$  i. e. when the aerofoil is placed between two solid walls,  $f_1 = 0$ ,  $f_2 = -\frac{1}{24}$ , and

$$\frac{L}{L_0} = \frac{1}{1 - \frac{k}{24} \left( \frac{\pi c}{b} \right)^2},$$

$L_0$  being the lift of an aerofoil in an unlimited uniform flow. And when  $x_1 = x_2 = \infty$  i. e. in the case of a free jet,  $f_1 = \frac{1}{2}$ ,  $f_2 = \frac{1}{12}$ , hence,

$$\frac{L}{L_0} = \frac{1}{1 + \frac{k}{2} \left( \frac{\pi c}{b} \right) + \frac{k}{12} \left( \frac{\pi c}{b} \right)^2}, \quad \frac{D}{L} = \frac{\Gamma}{2bV}.$$

When the exit edges of the upper and lower solid walls are not even with each other in the direction of  $x$ -axis, somewhat different conformal transformation is to be applied.

The case as shown in Fig. 3 will be explained here briefly. The exit edges are at  $x = -\frac{b}{2} \tan \gamma$ ,  $y = \frac{b}{2}$  and  $x = \frac{b}{2} \tan \gamma$ ,  $y = -\frac{b}{2}$  respectively, as shown in Fig. 3 (a). Though, in this figure, a vortex is placed at origin, the treatment applies to the vortex at any position. The flow in  $z$ -plane can be treated, as before, by considering a row of half infinite plates and a row of vortices as shown in Fig. 3 (b).  $z$ -plane is transformed into  $\zeta$ -plane by the following relations:

$$\begin{aligned} z &= \frac{b}{2\pi} \log \zeta_1, \quad \zeta_2 = \zeta_1 + im, \quad \zeta_3 = \zeta - \frac{a^2}{\zeta}, \\ z &= \frac{b}{2\pi} \log \left( \zeta - im - \frac{a^2}{\zeta} \right). \end{aligned} \quad (9)$$

For point A,

$$\zeta_{1A} = r_A e^{i\theta_A}, \quad \log r_A = -\frac{\pi}{2} \tan \gamma, \quad \theta_A = \frac{\pi}{2},$$

and for point B,

$$\zeta_{1B} = r_B e^{i\theta_B}, \quad \log r_B = \frac{\pi}{2} \tan \gamma, \quad \theta_B = -\frac{\pi}{2},$$

and

$$a = \frac{1}{4}(r_A + r_B) = \frac{1}{2} \cosh \left( \frac{\pi}{2} \tan \gamma \right),$$

$$m = \frac{1}{2}(r_A - r_B) = \sinh \left( \frac{\pi}{2} \tan \gamma \right).$$

The complex velocity potential of the flow is

$$\begin{aligned} F(z) &= Vz + F_1(z), \\ F_1(\zeta) &= \frac{i\Gamma}{2\pi} \log \frac{(\zeta - \zeta_0)(\zeta + \bar{\zeta}_0)}{(\zeta + \frac{a^2}{\zeta_0})(\zeta - \frac{a^2}{\bar{\zeta}_0})} + \frac{i\Gamma_s}{2\pi} \log \zeta - \frac{q}{\pi} \log \frac{\zeta - \zeta_e}{\zeta + \bar{\zeta}_e}, \end{aligned} \quad (10)$$

where  $\zeta_0$  is the point corresponding to  $O$  on  $z$ -plane,  $\bar{\zeta}_0$  the conjugate complex of  $\zeta_0$ ,  $\zeta_e$  the value of  $\zeta$  at point  $E_1$  corresponding to  $x = -\infty$  on  $z$ -plane and  $\bar{\zeta}_e$  the conjugate complex of  $\zeta_e$ .

The values of  $\Gamma_s$  and  $q$  are determined by the conditions that the velocities at A and B are not infinite. Generally, the value of  $q$  is not zero and hence,

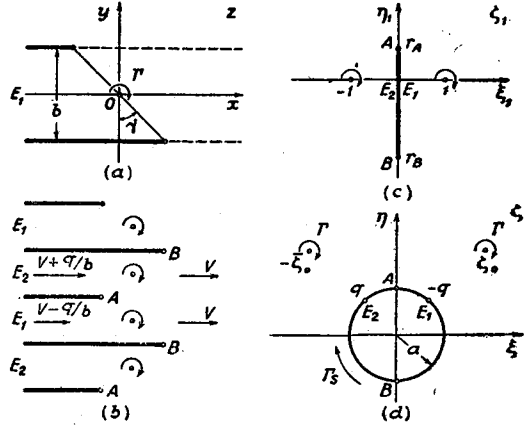


Fig. 3

the velocity at  $x = -\infty$  is  $V - \frac{q}{b}$ , while at  $x = \infty$  the velocity of free jet is equal to  $V$ .

Procedure of the further calculation is the same as in the previous case.

In the aerodynamic research of the wing cascade, such wind tunnels as shown in Fig. 4 are most widely used. Prof. G. Kamimoto<sup>2)</sup> applied the present method of calculation to this type of wind tunnels, replacing each aerofoil with single vortex, and the result thereby obtained is reproduced in Fig. 5. In this figure  $C_L$  indicates the lift coefficient measured by the wind tunnel,  $C_{L\infty}$  the corresponding lift coefficient of the wing cascade,  $n$  the number of aerofoils used in the wind tunnel,  $\gamma$  the angle of stagger and  $\lambda$  the pitch-chord ratio.

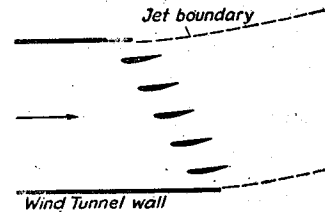


Fig. 4

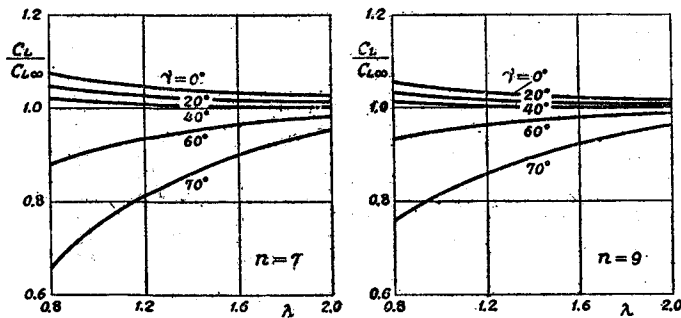


Fig. 5

## 2. Experiment

To test the validity of the above-mentioned theory, an experiment was made. We used a tiny wind tunnel of Göttingen type with square working

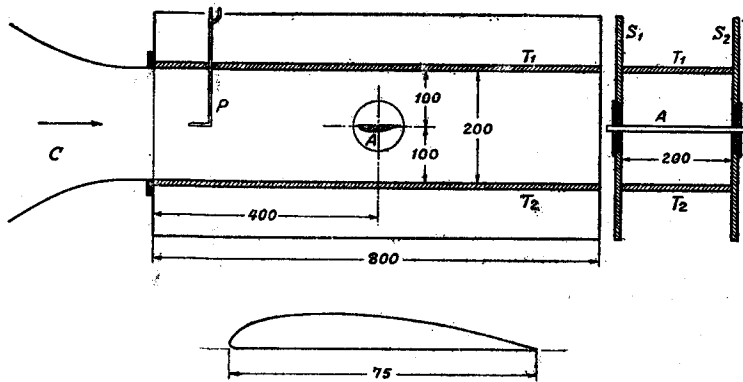


Fig. 6

section of 20 cm × 20 cm. The experimental section is attached to the entrance cone or nozzle  $C$  of the wind tunnel as shown in Fig. 6. This experimental section consists of two vertical plates  $S_1$  and  $S_2$  and two horizontal plates  $T_1$  and  $T_2$ .  $A$  is an aerofoil of 75 mm chord length and  $P$  is a Pitot tube. The experimental section has a length of 80 cm and the mid-chord point of the aerofoil is placed at 40 cm from its entrance. The lengths of the plates  $T_1$  and  $T_2$  were changed, unlike those of the plates  $S_1$  and  $S_2$  which were kept the same throughout the experiment.

The lift experienced by the aerofoil was estimated from the measured pressure distribution on the aerofoil. This method had to be applied owing to the lack of a balance, and accordingly the accuracy in the measurement of the lift had somewhat suffered.

Fig. 7 shows the measured value of lift coefficient  $C_L$ ,  $\alpha$  being the angle

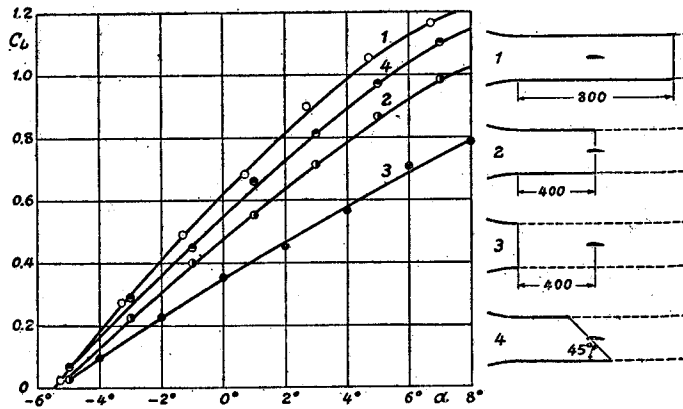


Fig. 7

of incidence. Experiment No. 1 deals with a case when the lengths of the plates  $T_1$  and  $T_2$  are 80 cm, i. e. the case of a closed type wind tunnel. Experiment No. 2 treats of a case when the lengths of plates  $T_1$  and  $T_2$  are 40 cm each and the mid-chord point of the aerofoil is at the exit of the closed tunnel. The case of a free jet is seen in Experiment No. 3, and Experiment No. 4 concerns a case when the exit of the tunnel is cut at an

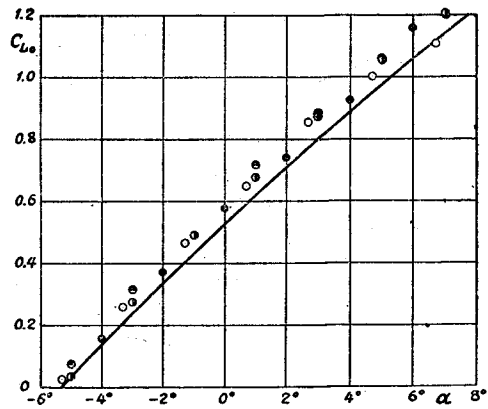


Fig. 8

angle of  $45^\circ$  and the  $c/4$  -point of the aerofoil is placed at the exit of the tunnel. Reynolds number is  $R = \frac{Vc}{\nu} \approx 10^5$ ,  $\nu$  being the kinematic coefficient of viscosity. In these cases the theoretical values of  $C_L/C_{L0}$ , where  $C_{L0}$  is the lift coefficient in a two-dimensional unlimited flow, are as follows:

Experiment	No. 1	No. 2	No. 3	No. 4
$C_L/C_{L0}$	1.052	0.816	0.610	0.920

The value of  $k$  is set at 0.86, which is determined by an experiment made by means of a much larger wind tunnel.

These experimental results are then corrected to the case of a two-dimensional unlimited flow and shown in Fig. 8. The points lie almost on a single curve. The line in this figure shows the value of a two-dimensional flow in a larger wind-tunnel. The value of  $c/b$  in this experiment is a little too large to apply the present theory. Yet from this experimental result, we may conclude that the theory is satisfactory.

Figs. 9 and 10 show the pressure difference between the upper and lower plates,  $T_1$  and  $T_2$ . Fig. 9 shows Experiment No. 1 in which  $C_L=1.06$ , and Fig. 10 No. 2, when  $C_L=0.80$ , the abscissae being  $x/b$  (see Fig. 1). In these figures, the theoretical values are also shown.

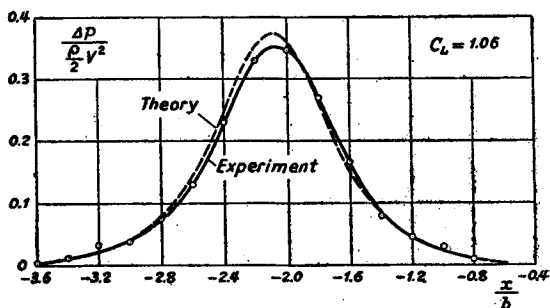


Fig. 9

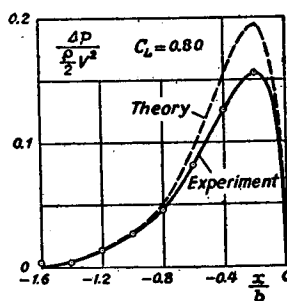


Fig. 10

Fig. 11 shows the boundary of a jet when  $C_L=0.66$ . The points show the positions where velocities are  $0.5V$ . The full lines show the theoretically calculated jet boundary. The broken lines in this figure are obtained as the locus of  $0.5V$  points when the estimation of the points are made

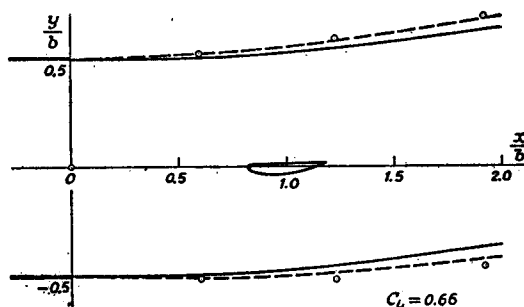


Fig. 11



according to the theory of Tollmien<sup>3)</sup>, taking into account of the possible spreading out of the jet boundary by turbulence.

#### **Conclusion**

In this paper, I have at first treated theoretically the interference effect of a wind tunnel partly composed of solid walls and partly of free boundary of a two-dimensional flow and then compared it with the experimental results. Coincidence between them is fairly perfect and it seems that this method can be extended to the wind tunnel interference of the wing cascade test.

#### **Acknowledgement**

The author expresses his cordial thanks to Mr. H. Dohata for his assistance in carrying out the experiments.

#### **References**

- 1) For example, see H. Glauert, Wind Tunnel Interference on Wings, Bodies and Airscrews, A. R. C. R. & M. No. 1566.
- 2) Kamimoto, G., Trans. of Japan Soc. Mech. Eng., Vol. 17, No. 58, 1951.
- 3) Tollmien, W., Z. A. M. M., Bd. 6, 1926.